Modeling and Control of Combustion Instability Using Fuel Injection [1]

J.P. Hathout, A.M. Annaswamy and A.F. Ghoniem
Department of Mechanical Engineering
Massachusetts Institute of Technology
Cambridge, MA 02139, USA

Abstract

Active control using periodic fuel injection has the po-
tential of suppressing combustion instability without
radically changing the engine design or sacrificing per-
formance. In this paper, we carry out a study of opti-
mal model-based control of combustion instability us-
ing fuel injection. The model developed is physically
based and includes the acoustics, the heat-release dy-
namics, their coupling, and the injection dynamics. A
heat-release model with fluctuations in the flame sur-
face area as well as in the equivalence ratio is derived.
We show that area fluctuations coupled with the veloc-
ity fluctuations drive longitudinal modes to resonance
caused by phase-lag dynamics, while equivalence ratio
fluctuations can destabilize both longitudinal and bulk
modes caused by time-delay dynamics, similar to ex-
perimental observations. The dynamics of proportional
and two-position (on-off) fuel injectors are included in
the model. Using the overall model, two different con-
trol designs are proposed. The first is an LQG/LTR
controller where the time-delay effect is ignored, and
the second is a Posi-Cast controller which explicitly ac-
counts for the delay. Injection at (i) the burning zone
and (ii) further upstream is considered. The character-
istics of fuel injectors including bandwidth, authority
(pulsed-fuel flow rate), and whether it applies a propor-
tional or a two-position (on-off) injection are discussed.
We show that increasing authority and bandwidth result
in improved performance. Injection at (ii) compared to
(i) results in a trade-off between improved mixing and
increased time-delay. We also note that proportional
injection is more successful than on-off injection since
the former can modulate both amplitude and phase of
the control fuel.

1 Introduction

Active control using periodic fuel injection has been
recognized as a promising technology to abate combus-
tion instability in practical systems [1]-[6]. Most cur-
rent designs are based on phase-shift algorithms which,
despite their success, are not optimal in terms of fuel
consumption, settling time, and robustness. Phase-shift
controllers, due to their limited dynamics, are known to
succeed only within a limited frequency band (around
the unstable frequency), and over a small range of op-
erating conditions. In this paper, we present alterna-
tive control designs using LQG/LTR and Posi-Cast con-
trol methods which are based on a physical model, and
demonstrate their advantages.

Control algorithms must be based on an accurate de-
scription of the system dynamics to achieve optimal
performance. Much effort has gone into modeling
acoustics [1],[7]-[10]. Modeling of heat-release dy-
namics and its coupling with acoustics, mixing dynam-
ics, and actuator dynamics, despite their crucial role in
the instability mechanism, have not been dealt with to
the same extent. Recognizing that heat-release oscilla-
tions can be caused by fluctuations of the flame surface
area due to velocity perturbation or the equivalence ra-
tio due to pressure perturbation, we derive a model that
incorporates both for the case of a weakly turbulent pre-
mixed flame. We show how certain acoustic modes can
couple with either or both forms of heat oscillations.

The feasibility of control design is tightly correlated
with the performance of sensors and actuators. While
high-bandwidth devices of the first are available, e.g.,
pressure transducers and heat-release sensors, actuation
by means of fuel injection is hindered by low band-
width, limited authority, and nonlinearities (in the form
of dead-zone, saturation and on-off effects) [11]. The
impact of ideal actuators was studied extensively in
[12]. The ability of the actuator to convey the control
signal faithfully to the combustor, thus introducing the
correct forcing, is key to stable performance. This how-
ever is often not the case due to (i) non-ideal injection

dynamics, and (ii) injection locations which may impose a delay in the control input. To capture the contribution of these effects in the control design, we develop a model of the injector dynamics and incorporate it in the overall analysis of the system.

In Sec. 2, we model the heat release dynamics forced by velocity and equivalence ratio fluctuations, the acoustic dynamics, the coupling and mixing dynamics, their effect on stability, and a generic model of typical solenoid injectors which captures its relevant features. In Sec. 3, control is developed for a multi-mode combustor and injection at as well as upstream of the burning zone is implemented. For the former, an optimal Linear-Quadratic Gaussian with Loop-Transfer Recovery (LQG/LTR) controller is used, and for the latter, a novel technique known as Posi-Cast control that accommodates combustion systems with delays is developed and implemented.

2 Combustor Model

Physically-based modeling has been shown to be indispensable for optimal control design for suppression of combustion instability [13]. The dynamics leading to combustion instability is known to occur due to the resonant coupling between acoustics and heat release. This coupling may occur through flame-area fluctuations, as shown experimentally in [1], and by modeling in [14]. It can also occur through mixture inhomogeneity (reactants' equivalence-ratio fluctuations), observed experimentally in [15]-[17], and modeled in [18, 19]. While both mechanisms can destabilize longitudinal modes [4, 7, 16, 20], bulk modes are more strongly affected by the latter [3, 18]. A rigorous model for the response of heat-release dynamics to these oscillations is shown next. This is followed by a description of acoustics, coupling mechanisms, and fuel-injector dynamics.

2.1 Heat-Release Dynamics

The response of the heat-release rate to perturbations in the flow velocity, u, as well the equivalence ratio, ϕ are modeled in this section. The flame kinematics equation is used to derive this model. The following assumptions are made: (i) The flame is a thin interface separating reactants and products and is insensitive to pressure perturbations [1]. The flame can model turbulent premixed combustion if conditions of high Damkohler number and weak to moderate turbulence intensity prevail [21]-[23]. (ii) The flame is weakly convoluted, i.e., it can be described by a single-valued function, $\xi(r,t)$, describing the instantaneous location of its surface.

Under the above assumptions, the heat-release model is

of the form [1]

$$\frac{\partial \xi}{\partial t} = u - v \frac{\partial \xi}{\partial r} - S_u(\phi)\sqrt{\left(\frac{\partial \xi}{\partial r}\right)^2 + 1}, \quad (1)$$

$$Q = \kappa(\phi) \int_0^R \sqrt{1 + \left(\frac{\partial \xi}{\partial r}\right)^2} \, dr, \quad (2)$$

where Q is the heat-release, S_u is the burning velocity, $\kappa(\phi) = 2\pi \rho_u S_u(\phi) \Delta h_r(\phi)$, ρ_u is the density of the unburnt mixture, and Δh_r is the heat of reaction.

Assuming negligible velocity component in the radial direction, and linearizing around nominal values $\overline{u}, \overline{S}_u$, and $\overline{\xi}(r)$, denoting $\overline{(.)}$ and $(.)'$ as steady and perturbation, respectively, we get

$$\frac{\partial \xi'}{\partial t} = u' + \overline{S}_u \frac{\partial \xi'}{\partial r} + \frac{\partial \overline{\xi}}{\partial r} \frac{dS_u}{d\phi}\bigg|_{\overline{\phi}} \phi', \quad (3)$$

with boundary conditions [2]

$$\xi'(R,t) = 0 \ \forall t, \qquad \xi'(r,0) = 0 \ \forall r,$$

while

$$Q'(t) = \overline{\kappa} \int_0^R \xi'(r,t)dr + d_1\phi', \quad (4)$$

where [3]

$$\overline{\kappa} = 2\pi \rho_u S_u \Delta \overline{h}_r,$$

$$d_1 = 2\pi \rho_u \left(\overline{S}_u \frac{d\Delta h_r}{d\phi}\bigg|_{\overline{\phi}} + \Delta \overline{h}_r \frac{dS_u}{d\phi}\bigg|_{\overline{\phi}}\right) \left(\int_0^R \overline{\xi}dr\right).$$

It is worth noting that the flame area fluctuation, A'_f, is given by $A'_f(t) = 2\pi \int_0^R \xi'(r,t)dr$. This with Eq. (3) shows that the flame area is affected by both u' and ϕ', and the area in turn impacts Q' as shown in Eq. (4). This also shows that ϕ' affects Q' directly, and indirectly through the area fluctuations.

Equation (3) can be manipulated further and solved for ξ' in the Laplace domain as:

$$\xi'(r,s) = \left(\frac{u'(s)}{s} + \frac{\partial \overline{\xi}}{\partial r} \frac{dS_u}{d\phi}\bigg|_{\overline{\phi}} \frac{\phi'(s)}{s}\right)\left(1 - e^{-(R-r)\frac{s}{\overline{S}_u}}\right), \quad (5)$$

where s is the Laplace operator. Differentiating Eq. (4) with respect to time, using Eq. (3), and integrating over $[0, R]$, we obtain that

$$\dot{Q}' = \overline{\kappa}\left(Ru' - \overline{S}_u \xi'(0,t) + \int_0^R \frac{\partial \overline{\xi}}{\partial r} \frac{dS_u}{d\phi}\bigg|_{\overline{\phi}} \phi'dr\right) + d_1\dot{\phi}'. \quad (6)$$

---

[1] We consider here a flame stabilized over a perforated plate. R is the radius of the perforation.

[2] It should be noted that with the appropriate change in coordinates and boundary conditions, Eq. (3) can also represent flames stabilized behind a gutter [24], or a dump [22].

[3] The factor $\frac{d\Delta h_r}{d\phi}\big|_{\overline{\phi}}$ is positive and $\frac{dS_u}{d\phi}\big|_{\overline{\phi}}$ is also positive when $\phi \leq 1$.

Taking the inverse Laplace of Eq. (5) at $r = 0$, and substituting in Eq.(6), after some manipulations, we get

$$\dot{Q}' = \bar{\kappa}\left(Ru' - \overline{S}_u \int_{t-\tau_f}^{t} u'(\tau)d\tau - \overline{S}_u d_2 \int_{t-\tau_f}^{t} \phi'(\tau)d\tau + d_3\phi'\right) + d_1\dot{\phi}', \qquad (7)$$

where

$$d_2 - \frac{d\bar{\xi}}{dr}\bigg|_0 \frac{dS_u}{d\phi}\bigg|_{\overline{\phi}}, \qquad d_3 - -\bar{\xi}(0)\frac{dS_u}{d\phi}\bigg|_{\overline{\phi}},$$

and $\tau_f = R/S_u$ is the characteristic propagation delay of the flame surface into the reactants flow. Note that for the class of flames considered in the paper, the slope at the flame tip, which is typically conical, is zero, therefore the third term in the RHS of Eq. (7) can be omitted.

The effect of u' on Q' was previously considered in [14] where the time-delay effects were assumed to be small. The effect of ϕ' on Q' was addressed in [18] where a lumped parameter approach was used where once again, the time-delay effects were neglected. In contrast, we have analyzed the effect of both perturbations on the flame dynamics where the impact of a time-delay, τ_f, is taken into account.

2.2 Acoustics

Acoustic resonance of a combustor can be captured by analyzing the wave equation and linearizing the conservation equations [20]

$$\frac{\partial^2 p'}{\partial t^2} - \bar{c}^2\frac{\partial^2 p'}{\partial x^2} = (\gamma - 1)\dot{q}'(x,t), \qquad (8)$$

where p is the pressure, and $\bar{c}$ is the mean speed of sound. We consider flames localized close to the anchoring plane, $q'(x,t) = q'(t)\delta(x - x_f)$.

Using an expansion in basis functions

$$p'(x,t) = \bar{p}\sum_{i=1}^{n} \psi_i(x)\eta_i(t), \qquad (9)$$

where in most cases, $\psi_i(x) = \sin(k_i x + \phi_{i0})$, k_i and ϕ_{i0} determined from the boundary conditions, and performing a weighted spatial averaging, the modal amplitudes can be shown to follow [20]:

$$\ddot{\eta}_i + 2\zeta\omega_i \dot{\eta}_i + \omega_i^2\eta_i = \sum_{i=1}^{n} \widetilde{b}_i \dot{q}'_f, \qquad (10)$$

where $\widetilde{b}_i = \gamma a_o\psi_i(x_f)/E$, $E = \int_0^L \psi_i^2(x)\,dx$, γ is the specific ratio, $a_o = \frac{\gamma-1}{\gamma\bar{p}}$, ζ represents the passive damping ratio in the combustor[4], L is its length, and $\omega_i = k_i\bar{c}$.

---

[4]Dissipation in a combustor can be caused by heat losses in the flame zone and friction due to viscous effects.

2.3 Coupling Dynamics

Perturbations in the flame area and the equivalence ratio which couple in a resonant way with the acoustic field are caused by velocity or pressure oscillations. Perturbations in the velocity and pressure are related to the perturbation in acoustic field via the energy equation [20]

$$\frac{\partial p'}{\partial t} + \gamma\bar{p}\frac{\partial u'}{\partial x} = (\gamma - 1)q', \qquad (11)$$

which can be integrated over the combustor length to obtain (using Eq. (9))

$$u' = \sum_{i=1}^{n} \widetilde{c}_i \dot{\eta}_i + \theta a_o q', \qquad (12)$$

where $\widetilde{c}_i = \frac{1}{\gamma k_i^2}\frac{d\psi_i}{dx}(x_f)$, $a_o = (\gamma - 1)/\gamma\bar{p}$, and θ represents the effect of the velocity ahead and behind the flame on q'. This equation can be used with Eq. (7) to couple the heat release to the velocity perturbations.

Perturbations in the equivalence ratio at the fuel source due to coupling with the acoustics can be modeled starting from the mass conservation at the mixing section which results in

$$\frac{\phi_s}{\overline{\phi}} \cong 1 \mp \frac{u'}{\overline{u}}, \qquad (13)$$

for fluctuations in the air flow only (fuel inlet is choked) or in the fuel flow only (air inlet is choked). Now using the momentum equation:

$$\bar{\rho}\frac{\partial u'}{\partial t} + \frac{\partial p'}{\partial x} = 0, \qquad (14)$$

and p' as in Eq. (9), after some manipulations, we get

$$\dot{\phi}_s' \cong \pm\overline{\phi}\frac{\bar{p}}{\overline{\rho u}}\sum_{i=1}^{n}\frac{d\psi_i(x)}{dx}\eta_i, \qquad (15)$$

according to fluctuations in the air flow only or in the fuel flow only. The equivalence ratio at the burning zone is related to that at the fuel source by a convective delay, $\tau_s = L_s/\overline{u}$, as

$$\phi' = \phi_s'(t - \tau_n), \qquad (16)$$

where $\tau_n = \tau_s + \tau_{comb}$, and the latter is the combustion time delay. In most cases $\tau_s \gg \tau_{comb}$, and hence $\tau_n \sim \tau_s$ is an acceptable approximation. We should also mention that in this analysis the radial distribution of the local equivalence ratio is assumed to be constant.

It is worth noting also that instability can arise in combustors where flue-gas recirculation is used to reduce NO_x formation, e.g. [25]. The recirculated products may couple with the acoustics and cause perturbations

in the equivalence ratio which can be described in a similar manner as in Eqs. (15) and (16). Also, when injection is used as actuation, it introduces an additional term to appear in the RHS of Eq. (16) and is discussed in Sec. 3.1.

2.4 The Overall Model

Combining the acoustics, heat-release dynamics, and convective-lag effects in Eqs. (10), (7) and (16), respectively, we obtain the following equations:

$$\ddot{\eta}_i + 2\zeta_i\omega_i\,\dot{\eta}_i + \omega_i^2\eta_i = \frac{\widetilde{b}_i}{A_c}\overline{\kappa}\{Ru' - \overline{S}_u\int_{t-\tau_f}^{t}u'(\tau)d\tau$$

$$+d_3\phi_s'(t-\tau_s)\} + d_1\,\dot{\phi}_s'\,(t-\tau_s),\quad (17)$$

where A_c is the cross-sectional area of the combustor. Equation (17) shows that two different time delays, τ_f and τ_s, can lead to instability, one arising from flame propagation effects, and the other from fuel convection. The RHS of Eq. (17) can be simplified further noting that for a certain class of flames τ_f is small when $\overline{S}_u$ is large (e.g., in a turbulent flow), and when the characteristic size of the flame, R, is small. Also, around the unstable acoustic frequency, $\dot{\phi}$ scales as $\omega|\phi|$, and $O(\overline{\kappa}d_3) \sim O(d_1)$, thus the second and third terms in the RHS can be neglected:

$$\ddot{\eta}_i + 2\zeta_i\omega_i\,\dot{\eta}_i + \omega_i^2\eta = \frac{\widetilde{b}_i}{A_c}\left[\overline{\kappa}Ru' + d_1\dot{\phi}_s'(t-\tau_s)\right].\quad (18)$$

The overall model of the combustor is represented by Eqs. (18), (12), and (15) when multiple modes are present. For ease of exposition, we restrict our discussion to the case when only one mode is present, a similar approach can be extended to the multi-mode case. Substituting for the coupling dynamics in Eqs. (12), (15) and (16), and assuming $\theta = 0$, we get

$$\ddot{\eta} + 2\zeta\omega\dot{\eta} + \omega^2\eta = \Gamma_1\dot{\eta} + \Gamma_2\eta'(t-\tau_s),\quad (19)$$

where $\Gamma_1 = \frac{\widetilde{bc}}{A_c}\overline{\kappa}R$ and $\Gamma_2 = \pm\frac{\widetilde{b}}{A_c}d_1\overline{\phi}\frac{\overline{p}}{\overline{\rho u}}\frac{d\psi^i(x)}{dx}$.

Defining the equivalent damping ζ_0 as

$$\zeta_o = \frac{2\zeta\omega - \Gamma_1}{2\omega}$$

when perturbations in the flame area change the equivalent damping in the combustor, such that $\zeta_o < 0$, the oscillator is always unstable. In this case, Γ_1 represents a "negative" damping added by the flame area fluctuations[5], and is suspected to cause the instability

---

[5]The notion of "negative" and "positive" damping is used here to indicate heat-release perturbation which is out-of-phase and in-phase with the pressure oscillation, respectively. We have shown in previous work [12] that the effect of flame-area perturbation can be modeled as a negative damping term. Heat release can be modulated using active forcing to produce a positive damping term, as shown in [19].

---

in [4, 26] where the reactants inlet were choked implying no ϕ' fluctuations. This condition arises when the flame is located in a position where the modal amplitude of the pressure and the velocity (represented by $\widetilde{b}$ and $\widetilde{c}$) are of the same sign. For example, in a closed-open combustor with fixed equivalence ratio, a quarter-wave mode is always stable whereas a three-quarter-wave mode gets destabilized when the flame is located between the node and the anti-node of the pressure mode [20].

If on the other hand, $\zeta_o > 0$, even though this implies that the damping is positive, perturbations in the equivalence ratio can destabilize the combustor due to the convective time-delay τ_s. When $\tau_s = 0$, the system is stable. As τ_s increases, the system becomes unstable if τ_s lies between τ_s^- and τ_s^+, where

$$\tau_s^{\mp} = \frac{1/\omega}{\sqrt{1 - 2\zeta_o^2 \pm \sqrt{\Gamma_2^2/\omega^4 - 4\zeta_o^2(1-\zeta_o^2)}}}$$

$$\times\ \cos^{-1}\left(\pm\frac{\sqrt{\Gamma_2^2/\omega^4 - 4\zeta_o^2(1-\zeta_o^2)} - 2\zeta_o^2}{\Gamma_2/\omega^2}\right),$$

if

$$2\zeta_o\sqrt{1-\zeta_o^2} < \frac{|\Gamma_2|}{\omega^2} < 1.$$

If $|\Gamma_2| > \omega^2$, there exists only one switch to instability at τ_s^-, though in most practical cases, we have $|\Gamma_2| < \omega^2$ [18].

When $\zeta_o \sim 0$, the above instability conditions simplify to [18, 19]: Defining the acoustic time constant $\tau_a = 2\pi/\omega$, the system is unstable if

$$\frac{n+1}{2} < \frac{\tau_s}{\tau_a} < \frac{n+2}{2}\qquad (20)$$

$n = 0, 2, 4...$, if $\Gamma_2 < \omega^2$, and unstable if $\frac{\tau_s}{\tau_a} > \frac{1}{2}$, if $\Gamma_2 > \omega^2$.

The above discussion indicates that the instability pattern depends on the distance between the source of ϕ_s', the convective velocity, and the acoustic frequency if perturbations in the equivalence ratio instigate the instability which appears to the instability mechanism in the rigs in [3, 16, 17]. The dependence of the stability bands on τ_s/τ_a can be judiciously exploited for optimizing the active-control designs [19].

2.5 Fuel Injector Dynamics

2.5.1 A Proportional Injector: The pulsating fuel injector delivers oscillations in the mass-flow rate in response to a voltage input. The injector system consists of an electro-mechanical part and a fluidic part, where in the former, the input voltage generates an
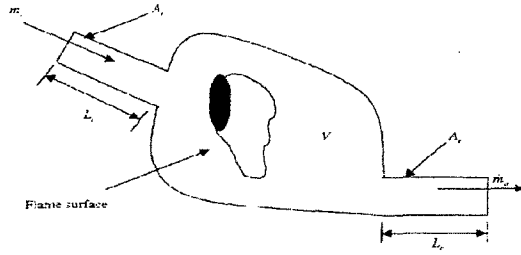
Figure 1: A schematic of a typical injector.

electro-magnetic field that causes a poppet to move against a spring (as seen in Fig. 1). The motion of the poppet controls the aperture of the injector allowing fluid to flow.

The electro-mechanical part relates the voltage E to the poppet position x through the electrical, electro-magnetic, and mechanical components, which can be modeled as

$$E = iR_e + L_e \frac{di}{dt} + V, \quad (21)$$

$$V = B_e l \frac{dx}{dt}, \quad (22)$$

$$F_m = B_e l i, \quad (23)$$

$$m \frac{d^2x}{dt^2} + b \frac{dx}{dt} + kx = F_m, \quad (24)$$

where i is the current, F_m is the magnetic force, x denotes the motion of the armature in the direction of the magnetic force, R_e, L_e, B_e, and l denote, the resistance of the solenoid coil, the inductance of the coil, the magnetic flux density, and the length of the armature which moves orthogonal to the magnetic field, respectively. m, b, and k represent the effective mass, damping, and the stiffness of the armature/poppet system.

The fluidic part can be modeled using the unsteady Bernoulli equation, and the conservation of mass across the injector assuming incompressible flow. The unsteady velocity, v, can be obtained from the former applied between the inlet to the valve which is connected to a pressurized tank (where the flow velocity is ≈ 0, and $p = p_o$), and the outlet to the combustor where $p = p_c$, and $\Delta p = p_o - p_c$, as

$$\rho L_i \frac{dv}{dt} + \frac{1}{2}\rho v^2 = \Delta p, \quad (25)$$

In case small perturbations in p_c affect the velocity out of the injector, the unsteady velocity out of the valve, v, is linearized as

$$\tau_{fluid} \frac{dv'}{dt} + v' \cong \frac{-p'_c}{\sqrt{2\Delta \bar{p} \rho}}, \quad (26)$$

where $\tau_{fluid} = L_i/\sqrt{2\Delta\bar{p}/\rho}$ is the fluidic time constant, and L_i is the distance between the tank and the

valve's outlet. τ_{fluid} is negligible for conditions where $L_i \ll 1m$, $\Delta\bar{p}$ is large (which is expected), and ρ is small ($O(1kg/m^3)$ for most gaseous fuels)[6].

The mass flow rate, defined as $\dot{m}_f = \rho v A$, is perturbed, assuming oscillations in v (caused by the dynamics in Eq. (26)) and A (caused by the motion of the poppet x), as

$$\dot{m}'_f = \rho \bar{A} v' + \rho \bar{v} A', \quad (27)$$

where we assume $A' = k_o x$, and $k_o > 0$. Equations (26) and (27) describe the fluid dynamics due to perturbations in p'_c and/or x. In most practical cases, $\Delta\bar{p}$ is large to guarantee choked conditions in the injector's discharge, thus, the first term in the RHS of Eq. (27) can be neglected. Using $\bar{v} = \sqrt{\frac{2\Delta\bar{p}}{\rho}}$ from Eq. (25), we simplify Eq. (27) as

$$\dot{m}'_f \cong k_o \rho \sqrt{\frac{2\Delta p}{\rho}} x. \quad (28)$$

Equations (21)-(24) and (28) determine the input-output relation between the fuel-injector input E and the output $\dot{m}'_f$ which is expressed in the Laplace domain as:

$$\frac{\dot{m}'_f(s)}{E(s)} = \frac{k_v}{(\tau_e s + 1)(ms^2 + bs + k) + B_e^2 l^2/R_e s}, \quad (29)$$

where $k_v = B_e l k_o \rho \sqrt{\frac{2\Delta\bar{p}}{\rho}}/R_e$.

In most solenoid systems, the armature electric time constant, $\tau_e = L_e/R_e$, is negligible compared to the acoustics time constant [27]. In these valves, the stiffness of the spring, k, is large, for a fast closing of the valve, when the voltage is turned *off*. Also, the mass, m, of the armature is very small in many of the typical injectors to minimize inertia forces [27]. The damping term, b, contains the overall damping including stiction and friction, and typically is large. Thus, the mechanical system can be simplified as a first-order system; a damper-spring system [28]. The mechanical time constant usually limits the bandwidth of typical injectors to approximately 100 Hz. (Note that other effects, such as impact dynamics are not included here, since we expect them to be of higher frequencies than the combustor dynamics). Thus, Eq. (29) is simplified as

$$\frac{\dot{m}'_f(s)}{E(s)} = \frac{k_v \tau_m}{\tau_m s + 1}, \quad (30)$$

where $\tau_m = (b + B_e^2 l^2/R_e)/k$.[7]

---

[6] In the case of liquid fuels, the time constant can be comparable to the acoustics time constant due to large ρ, $O(1000kg/m^3)$.

[7] For more advanced proportional injectors, internal feedback loops exist (using for example a position transducer for the armature) to guarantee accurate metering, and increase its bandwidth, e.g., a Moog DDV proportional valve has a bandwidth of 450 Hz [29].
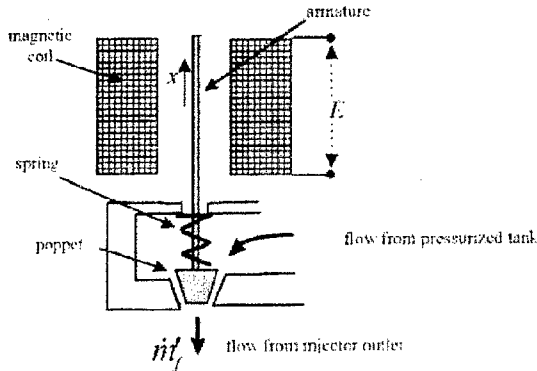
Figure 2: Block diagram of a typical two-position injector.

2.5.2 A Two-Position (on-off) Fuel injector:

Some fuel injectors currently used for combustion control [6, 11, 30] operate only between two positions, *on* and *off*. Unlike the proportional injectors discussed above, the physical stops play a more prominent role in the dynamics. However, one can still model two-position injectors in the same manner as above by including the effect of the physical stops as a saturation block together with Eq. (30) as shown in Fig. 2. A two position injector is set *on*, after the voltage input overcomes a certain threshold, thus creating a dead-zone in the control input (see figure) which will be discussed further when control is implemented in Sec. 3.

An additional point to note is the distinction between the injector dynamics during transition from closing and opening. Typically, the injector is over-driven by a high voltage in the opening mode to ensure fast opening. The opening time constant is different than the closing one. This effect can also be included in the injector model, as seen in Fig. 2, by assuming that τ_m varies between two values τ_{m_1} and τ_{m_2} depending on whether the injector is transitioning from *off* to *on* or *on* to *off*. Note that $\tau_{m_1} = \tau_m$ (as defined before) and $\tau_{m_2} = b/k$. We refer the reader to [31] for more details regarding this model when validated against two different Parker-Hannafin Series-9 injectors *9-130-905* and *9-633-900*.[8]

3 Control

In this section, we investigate model-based control strategies for abating combustion instability using sec-

---

[8]It should be noted that when inertia forces in the armature are important, a second-order fuel-injector model, with high damping, is more appropriate. The experimental measurements in [30] for a General Valve injector show similar dynamics.

ondary fuel injection. We assume that the pressure signal is the measured output, using a pressure transducer. The transducer dynamics is neglected since it typically has a much higher bandwidth than the combustion dynamics. We examine the control with an injector located at (i) the burning zone or (ii) further upstream. We assume in particular that the combustion dynamics is determined by several coupled acoustic modes [20]. We also assume that instability is primarily induced by fluctuations in the flame area coupled with the acoustics. We refer the reader to [18, 19] for investigations of instability caused by equivalence ratio fluctuations and its control.

3.1 Actuated Combustor

Denoting the contribution of the fuel injector to the equivalence ratio as ϕ'_c, we have that $\phi'_c = \frac{m'_f}{\overline{m}_a}/\alpha_o$, where $\overline{m}_a$ and α_o are the mean air mass flow rate, and the stoichiometric fuel to air ratio, respectively. We assume that ϕ'_c is uniform radially, and that perturbations are carried intact by the mean flow to the burning zone, after a time delay τ_c, where $\tau_c = L_c/\overline{u}$. L_c is the distance between the injector discharge and the burning zone, and $\overline{u}$ is the mean velocity of the reactants in the combustor.

From Eq. (18), the impact of ϕ'_c on the combustion dynamics can be taken into account as

$$\ddot{\eta}_i + 2\zeta\omega_i\,\dot{\eta}_i + \omega_i^2\eta - \frac{\overline{b}_i}{A_c}\left[\overline{\kappa}Ru' + d_1\dot{\phi}_c(t - \tau_c)\right], \quad (31)$$

for $i = 1, 2, .., n$, where i denotes the mode number.

3.2 Injection at the Burning Zone

Injection at the flame has shown success in several experimental facilities [6, 11, 30], and in a practical full-scale 170 MW gas-turbine combustor [5]. We carry out active control design assuming that the injection is at the flame, using the model in Eq. (31) while $\tau_c \approx 0$, together with the injection dynamics described by Eq. (30). The input-output model relation between the injector input voltage, E, and the pressure, p', is given by

$$p'(s) = W_p(s)E(s), \qquad W_p(s) = \frac{k_p Z_p(s)}{R_p(s)}. \quad (32)$$

where $W_p(s)$ is the transfer function of a finite-dimensional model of the combustor. k_p, $Z_p(s)$ and $R_p(s)$ are the corresponding gain, numerator and denominator, respectively.

An optimal control for the finite-dimensional system as in Eq. (32) is LQG/LTR [32]. This method has been successful in suppressing combustion instability

[13]. Its success lies in its ability to generate satisfactory performance over a wide range of frequencies, unlike phase-shift controllers which can destabilize stable dynamics [33]. Experimental validation of the LQG/LTR for combustion control has been demonstrated in [31, 34, 35]. In [34], a similar physically-based model was used with a loudspeaker as an actuator. In [31, 35], a system-ID approach based on subspace and ARMAX methods [36] was used to suppress pressure oscillations in a dump and a swirl-stabilized combustors, respectively, using pulsed injection. In this paper, we show through simulation studies that, as in [13], LQG/LTR can also be used successfully based on a physical model, using fuel injector as an actuator. For details of the LQG/LTR control design, we refer the reader to [13, 34].

3.2.1 Simulations of the LQG/LTR Controller:

A fifth order combustor dynamics model including the first two modes, the flame dynamics, and the injector dynamics is considered. The combustor parameters and conditions are taken as in [13], these cause a three-quarter-mode instability which resonates at 500 Hz approximately, and has unsteady pressure amplitudes of $O(100Pa)$.

We choose first a proportional injector, as in [5], with a bandwidth of 300 Hz which is in the range of available high-speed injectors [29]. Figure 3 shows the time response of the pressure and the control input, $\phi'_c/\overline{\phi}$ ($\overline{\phi} = 0.7$). Control is applied at $t = 50ms$. We note that although the bandwidth is lower than the system dynamics, the control with proportional injector is still capable of stabilizing the system, since the dynamics of the injector are taken into consideration in the design of the LQG/LTR. As seen in Eq. (30), the injector dynamics are first order, and the gain and phase introduced by the injector depend on its bandwidth. For smaller bandwidths cases, the phase increases while the control authority, i.e., the gain, is dramatically decreased around acoustic frequencies. The controller, however, has enough degrees of freedom to adjust the phase, and increase the voltage amplitude into the injector to produce the required control authority, $\phi'_c/\overline{\phi}$, around the acoustics frequencies thus guaranteeing stability.

While a low bandwidth proportional injector is capable of maintaining the system at vanishingly small pressure perturbations, a two-position injector may not be as effective [11, 30, 35]. Using a 300 Hz bandwidth injector, the LQG/LTR is still capable of stabilizing the system, but the pressure is suppressed to a small but finite amplitude limit cycle as seen in Fig. 4. The reason is that the injector has a threshold input voltage value at which it is activated. Thus, following the suppression of the instability, the injector stops pulsing at from
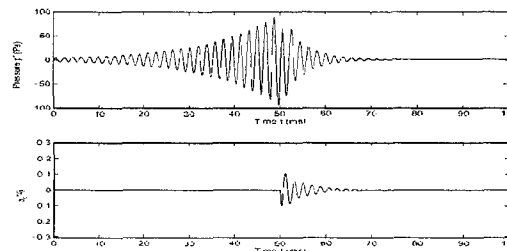

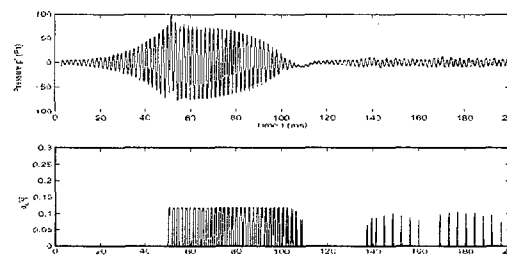**Figure 3:** Response of the controlled combustor with a proportional injector with a bandwidth of ≈ 300 Hz.

Figure 4: Response of the controlled combustor with an on-off injector set to deliver $\frac{\phi_c|_{max}}{\overline{\phi}} \approx 0.125$ and with a bandwidth ≈ 300 Hz.

$t \approx 105$-$138ms$, as seen in the figure. Disturbances in the combustor force the pressure to grow, until the measured voltage by the microphone reaches the threshold at which the injector starts to fire again. In the case simulated, this occurs at $t > 138ms$. This sequence is repeated indefinitely.

Increasing the control fuel-flow rate, and thus $\phi_c|_{max}$, the combustor is stabilized in a smaller settling time. As seen in Fig. 5, when $\phi'_c|_{max}/\overline{\phi}$ is doubled, the settling time diminishes by $\sim 80\%$. Moreover, the rms of the steady-state pressure is smaller. A similar effect has been observed in [11].

We also investigate the effect of bandwidth for a two-position injector. Limiting it to 50 Hz, as seen in Fig. 6, the pressure settles to a higher-amplitude limit cycle, and the injector is incapable of tracking the command
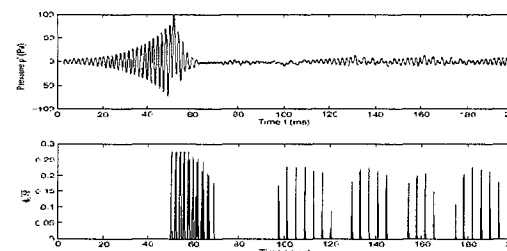

Figure 5: Response of the controlled combustor with on-off injector set to deliver $\frac{\phi_c|_{max}}{\overline{\phi}} \approx 0.27$, and with a bandwidth of 300 Hz.
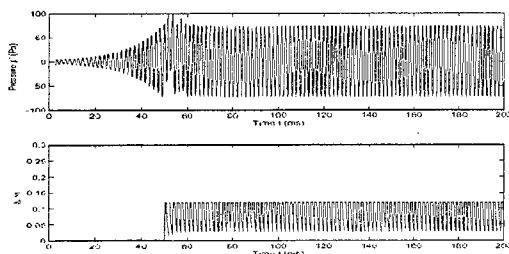
Figure 6: Response of the controlled combustor with on-off injector with lower bandwidth ≈ 50 Hz (the acoustics unstable frequency is 500 Hz, approximately).

from the controller; the injector stays open all the time. This shows that injector bandwidth is a serious problem [11, 35]. Different solutions have been proposed that include: (i) Developing faster injectors [29]. (ii) Use of multiple injectors which are fired alternatively to increase the apparent frequency of actuation [11]. A different approach that has shown promise regardless of high-bandwidth injectors is through fuel pulsing at low frequencies (much lower than the acoustics). This is demonstrated experimentally in [4, 37], and analytically in [38].

3.3 Injection Upstream the Burning Zone: Delay in the Control Input

While injecting fuel directly on the flame [5, 6, 11, 30] can avoid actuation delays, it introduces hot spots at the flame surface thus increasing emissions. In addition, if mixing is weak at the injection port, we run the danger of creating a secondary diffusion flame which can be completely decoupled from the main premixed flame, and hence become ineffective in suppressing the instability [9].

In this section, we study the effects of pulsed-fuel injection upstream the burning zone. This has been utilized in [3] where secondary injection was done at the primary fuel source. In [19], we presented a Posi-Cast control capable of working with an injector located at an arbitrary distance upstream the flame. In that case, a bulk mode was unstable. Here, we extend the analysis of the Posi-Cast control, and show that it is capable of stabilizing longitudinal modes as well.

3.3.1 Posi-Cast Control: A powerful approach for controlling systems with known time-delay was originated by Smith [40], known also as Posi-Cast for "positive forecasting" of future states. The idea is to compensate for the delayed output using input values stored over a time window equal to the delay time, i.e. $[t - \tau_c, t]$, and estimate the future output using a model

---

[9]This has been noticed in experiments at MIT and at UTRC [39].

of the combustor. Only stable systems were considered. An extension to include unstable systems was proposed in [41] using finite-time integrals of the delayed input values thereby avoiding unstable pole-zero cancellations which may occur. A frequency-domain pole-placement technique for unstable systems was first proposed in [42] and a similar technique will be presented here.

The model in Eq. (32), in the presence of a time delay, τ_c, can be re-written as

$$p'(t) = W_p(s)[E(t - \tau_c)], \qquad W_p(s) = \frac{k_p Z_p(s)}{R_p(s)} \quad (33)$$

Due to the nature of the combustion system, not all states are accessible, only the system input, i.e. the voltage to the injector $E(t)$, and the output, p' in our case are measured. A standard pole-placement controller is required (for more information, see [42, 43]). The presence of the time-delay, τ_c, in the control input, motivates the use of an additional signal in the control input, $E(t)$, denoted as $E_1(t)$ which anticipates the future output using a model of the system [19]. The resulting controller structure is described as

$$E(t) = \frac{c(s)}{\Lambda(s)} E(t - \tau_c) + \frac{d(s)}{\Lambda(s)} p'(t) + E_1(t),$$
$$(34)$$

$$E_1(t) = \frac{n_1(s)}{R_p(s)} E(t) - \frac{n_2(s)}{R_p(s)} E(t - \tau_c),$$

where $\Lambda(s)$ is a chosen stable polynomial of degree $n - 1$, $d(s), n_1(s)$ and $n_2(s)$, are polynomials of degree $n - 1$ at most, and $c(s)$ is of degree $n - 2$ at most. For stability, these must satisfy the relations

$$c(s)R_p(s) + k_p d(s)Z_p(s) = \Lambda(s)n_2(s), \quad (35)$$
$$n_1(s) = R_p(s) - R_m(s) \quad (36)$$

where $R_m(s)$ is the desired characteristic equation, which is a stable monic polynomial of the same order of $R_p(s)$.

Using the controller structure in Eq. (34) with the conditions in Eqs. (35) and (36), the closed-loop transfer function can be computed as

$$W_{cl}(s) = \frac{k_p e^{-s\tau_c}}{R_m(s)}. \quad (37)$$

The control input law, in Eq. (34), introduces additional dynamics including non-minimum phase zeros having the same eigen-values of $R_p(s)$. Obviously, these lead to unstable pole-zero cancellations since the combustor model is open-loop unstable (i.e., $R_p(s)$ has unstable eigen values). Unstable pole-zero cancellations are
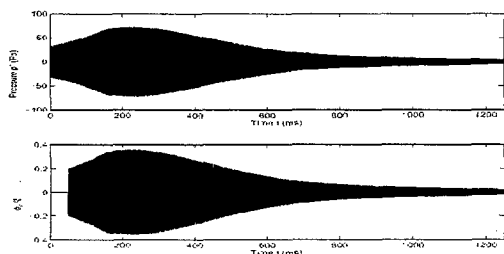
Figure 7: Response of the controlled combustor with a time-delay of 100ms in the input signal, proportional injector. Note: only the envelope of the response is shown for clarity, since the scale of the plot does not permit seeing individual cycles.

Figure 8: Response of the controlled combustor with a time-delay of 100ms in the input signal, on-off injector. Note: only the envelope of the response is shown for clarity, since the scale of the plot does not permit seeing individual cycles.

known to cause problems concerning observability and controllability of the plant (see [27] for more details). As a result, a modification in the synthesis of $E_1(t)$ in Eq. (34) was suggested by [41]. To avoid unstable pole-zero cancellations, $E_1(t)$ must be generated as a finite integral of the form

$$ E_1(t) = \sum_{i=1}^{n} \left(\int_{-\tau_c}^{0} e^{-\lambda_i \sigma} E(t + \sigma) d\sigma \right), \quad (38) $$

where λ_i's are the eigen values of the combustor system, i.e. $R_p(s) = \Pi_{i=1}^{n}(s - \lambda_i)$. Taking the Laplace transform of Eq. (38), one can show that

$$ \frac{n_1(s)}{R_p(s)} = \sum_{i=1}^{n} \frac{\alpha_i}{s - \lambda_i}, \frac{n_2(s)}{R_p(s)} = \sum_{i=1}^{n} \frac{\beta_i}{s - \lambda_i}, \quad (39) $$

where $\beta_i = \alpha_i e^{\lambda_i \tau_c}$. Another condition for the successful use of the finite integral in Eq. (38) is that $R_p(s)$ has no repeated roots [42].

The controller described in Eqs. (34) and (38) is sufficient to stabilize the combustor provided that an accurate description of the plant and the time delay are available. This controller has been shown to provide robustness to uncertainties in the plant including the time delay [41]. Adaptive versions of the same controller have been investigated [44, 45], and have shown to extend the robustness of the controller to parameter uncertainties.

3.3.2 Simulations of the Posi-Cast Controller:
The controller in Eqs. (34) and (38) is implemented for injection at a distance of $\sim 3cm$ upstream the burning zone. τ_c is estimated to be 100ms, which is about 50 times the time constant of the unstable frequency.

The closed-loop simulation is illustrated in Fig. 7. Although control is switched on at $t = 50ms$, the pressure keeps increasing for an additional $t = \tau_c = 100ms$ (from $t = 50 - 150ms$), then stalls for another 100 ms (from $t = 150 - 250ms$) before decaying. The reason
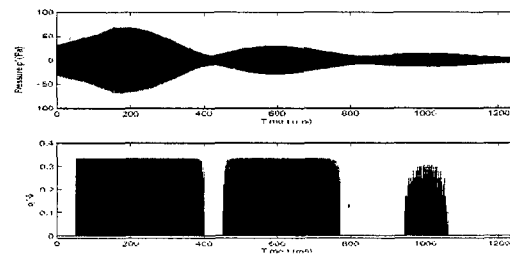
for the former delay is physical and is due to the time taken for the pulsed-fuel to reach the burning zone. The latter is due to a computational delay in the controller. Specifically, the finite integral in Eq. (38) outputs incorrect values for a period of τ_c. This is because the computation of the finite integral relies on a stored window of the past values of the control input of the size of τ_c. When control is switched on, the window consists of control inputs proportional to p' which has not yet "felt" the effect of control due to the physical delay τ_c (the values of p' are still those of the open-loop combustor). It requires therefore $t = 2\tau_c$ to start forming a window of integration with control input corresponding to closed-loop values. This confirms observations in [41].

In Fig. 8, a two-position injector is used. The control design is based on the linear model, and its parameters are fine-tuned to handle the nonlinearities. As discussed earlier, the control is switched on at 50ms, and stabilizes the system. The injector stays on as long as the voltage signal into the injector is greater than a threshold, as discussed before in Sec. 2.5.2.

It should be noted that when combustion instability is caused by ϕ_s' fluctuations, as discussed in Sec. 2, the characteristic equation will look different than in Eqs. (32) and (33). $R_p(s)$ will have terms which are delayed, due to the convective delay, τ_s, carried by ϕ_s'. Hence, $R_p(s)$ becomes infinite dimensional. To circumvent this, a Padé approximation [46] is used to get a finite dimensional description of $R_p(s)$, and thus the LQG/LTR and Posi-Cast controllers as described in Secs. 3.2 and 3.3, respectively, can similarly be used for this case.

4 Summary

In this paper, a complete model of the combustion dynamics leading to instability is developed. A model encompassing the acoustics, the heat release, the cou-

pling, mixing and injector dynamics is presented. The heat release is derived using flame kinematics for flames with high Damkohler numbers and moderate turbulence, and the effect of forcing in the velocity and the equivalence ratio is illustrated. Different stability criteria are discussed for the different dynamics resulting from the coupling of these with the acoustics. While velocity perturbations cause instability of a phase-lag nature, equivalence-ratio oscillations introduce a time-delay instability. Injection both at and upstream of the burning zone is studied. An LQG/LTR control is used for the former while a Posi-Cast control is developed and used for the latter. Both proportional and two-position (on-off) pulsed injection is examined. Proportional injectors show superior performance to two-position ones. Performance is shown to be plagued by limited injector authority and bandwidth. Some of the short-term fixes proposed for this problem include the use of multiple injectors [11] and low frequency pulsing [4, 37, 38]. A long-term solution is clearly the design of a high-speed, high-authority injector.

References

[1] G. J. Bloxsidge, A. P. Dowling, N. Hooper, and P. J. Langhorne. Active control of an acoustically driven combustion instability. *Journal of Theoretical and Applied Mechanics*, supplement to vol. 6, 1987.

[2] K.R. McManus, T. Poinsot, and S.M. Candel. A review of active control of combustion instabilities. *Progress in energy and combustion science*, 19(1):1–30, 1993.

[3] J. M. Cohen, N. M. Rey, C. A. Jacobson, and T. J. Anderson. "Active control of combustion instability in a liquid-fueled low-NOₓ combustor". *ASME 98-GT-267, ASME/IGTI, Sweden*, 1998.

[4] G. A. Richards, M. C. Yip, and E. H. Rawlins. Control of flame oscillations with equivalence ratio modulation. *Journal of Propulsion and Power*, 15:232–240, 1999.

[5] J.R. Seume, N. Vortmeyer, W. Krause, J. Hermann, C.-C Hantschk, P. Zangl, S. Gleis, and D. Vortmeyer. "Application od active combustion instability control to a heavy duty gas turbine". In *Proceedings of the ASME-ASIA, Singapore*, 1997.

[6] S. Murugappan, S. Acharya, E. Gutmark, and T. Messine. "Active control of combustion instabilities in spray combustion with swirl". *AIAA-2000-1026, 38th AIAA Aerospace Sciences Meeting, Reno, NV*, 2000.

[7] W. Lang, T. Poinsot, and S. Candel. Active control of combustion instability. *Combustion and Flame*, 70:281–289, 1987.

[8] F. E. C. Culick. Nonlinear behavior of acoustic waves in combustion chambers. *Acta Astronautica*, 3:715–756, 1976.

[9] B.T. Zinn. *Pulsating combustion. Advanced Combustion Methods*. Academic Press Inc. (London) LTD., London, 1986.

[10] V. Yang, A. Sinha, and Y.-T. Fung. State feedback control of longitudinal combustion instabilities. *Journal of Propulsion and Power*, 8, 1992.

[11] K. Yu, K.J. Wilson, and K.C. Schadow. Scale-up experiments on liquid-fueled active combustion control. In *34th AIAA/ASME/SAE/ASEE Joint Propulsion Conference*, pages AIAA 98-3211, Cleveland, OH, 1998.

[12] J. P. Hathout, M. Fleifil, A. M. Annaswamy, and A. F. Ghoniem. Role of actuation in combustion control. In *1999 IEEE CCA/CACSD*, Hawai'i, August 22-27 1999.

[13] J. P. Hathout, A. M. Annaswamy, M. Fleifil, and A. F. Ghoniem. Model-based active control design for thermoacoustic instability. In *Combustion Science and Technology*, volume 132, pages 99–138, 1998.

[14] M. Fleifil, A. M. Annaswamy, Z. Ghoniem, and A. F. Ghoniem. Response of a laminar premixed flame to flow oscillations: A kinematic model and thermoacoustic instability result. *Combust. Flame*, 106:487–510, 1996.

[15] A.A. Putnam. *Combustion Driven Oscillations in Industry*. American Elsevier Pub. Co., NY, 1971.

[16] G.A. Richards and M.J. Yip. Oscillating combustion from a premix fuel nozzle. *The Combustion Institute/American Flame Research Committee Meeting, San Antonio TX*, 1995.

[17] T. Lieuwen and B.T. Zinn. "The role of equivalence ratio oscillations in driving combustion instabilities in low NOₓ gas turbines". *The Twenty Seventh International Symposium on Combustion*, pages 1809–1816, 1998.

[18] M. Fleifil, J.P. Hathout, A.M. Annaswamy, and A.F. Ghoniem. "Reduced order modeling of heat release dynamics and active control of time-delay instability". *AIAA 2000-0708, 38th AIAA Aerospace Sciences Meeting, Reno, NV, 10-13 January*, 2000.

[19] J. P. Hathout, M. Fleifil, A. M. Annaswamy, and A. F. Ghoniem. Heat-release actuation for control of mixture-inhomogeneity-driven combustion instability. In *28ᵗʰ International Symposium on Combustion*, University of Edinburgh, Scotland, July 30-August 4 2000.

[20] A. M. Annaswamy, M. Fleifil, J. P. Hathout, and A. F. Ghoniem. Impact of linear coupling on the design of active controllers for thermoacoustic instability. *Combust. Sci. Tech.*, 128:131–180, 1997.

[21] H.M. Najm and A.F. Ghoniem. "Modeling pulsating combustion in vortex stabilized pre-mixed flames". *Combustion Sci. Tech.*, 94:259–278, 1993.

[22] A. A. Peracchio and W. Proscia. Nonlinear heat release/acoustic model for thermoacoustic instability in lean premixed combustors. In *ASME Gas Turbine and Aerospace Congress*, Sweden, 1998.

[23] A.P. Dowling. "A kinematic model of of a ducted flame". *Journal of Fluid Mechanics*, 394:51–72, 1999.

[24] A. P. Dowling. Nonlinear acoustically-coupled combustion oscillations. *2nd AIAA/CEAS Aeroacoustics Conference*, May 6-8 1996.

[25] J.D. Anderson. *Fundamentals of Aerodynamics*. McGraw-Hill, Inc., New York, 1991.

[26] K.K. Venkataraman, L.H. Preston, D.W. Simons, B.J. Lee, J.G. Lee, and D.A. Santavicca. "A study of the mechanism of combustion instability in a lean premixed dumb combustor". *Submitted to the Journal of Power and Propulsion*, 1998.

[27] K. Ogata. *Modern Control Engineering*. Third Edition, Prentice Hall, Inc., NJ, 1997.

[28] L. Meirovitch. *Elements of Vibration Analysis (Second Edition)*. McGraw-Hill, Inc., NY, 1986.

[29] C. Hantschk, J. Hermann, and D. Vortmeyer. "Active instability control with direct drive servo valves in liquid-fuelled combustion systems". In *Proceedings of the International Symposium on Combustion*, Naples, Italy, 1996.

[30] J.C. Magill, M. Bachmann, and K.R. McManus. Combustion instabilitydynamics and control in liquid-fueled direct injection systems suppression in liquid-fueled combustors. *38th Aerospace Sciences Meeting and Exhibit*, AIAA-2000-1022, 2000.

[31] B. J. Brunell. "A system identification approach to active control of thermoacoustic instabilities". In *S.M. Thesis*, MIT, Cambridge, MA, 2000.

[32] G. Stein and M. Athans. The LQG/LTR procedure for multivariable feedback control design. *IEEE Transactions on Automatic Control*, 32:105–114, 1987.

[33] M. Fleifil, J. P. Hathout, A. M. Annaswamy, and A. F. Ghoniem. The origin of secondary peaks with active control of thermoacoustic instability. *Combustion, Science, and Technology*, 133:227–265, 1998.

[34] A. M. Annaswamy, M. Fleifil, J. Rumsey, R. Prasanth, J. P. Hathout, and A. F. Ghoniem. Thermoacoustic instability: Model-based optimal control and experimental validation. *IEEE Control Systems Technology*, vol. 8, pp. 905-918, November 2000.

[35] S. Murugappan, S. Park, S. Acharya, A.M. Annaswamy, E. Gutmark, and A.F. Ghoniem. "Optimal control design for a swirl-stabilized combustor using system identification methods". *38th Aerospace Sciences Meeting and Exhibit*, AIAA-2001-0779, Reno, NV, January 2001.

[36] L. Ljung. *System Identification: Theory for the User*. Prentice-Hall, Englewood Cliffs, NJ, 1987.

[37] S. Sivasegaram and J. H. Whitelaw. Active control of oscillations in combustors with several frequency modes. In *Proceedings of the ASME Winter Annual Meeting*, Anaheim, CA, 1992.

[38] R. Prasanth, A.M. Annaswamy, J.P. Hathout, and A.F. Ghoniem. "When do open-loop strategies for combustion control work?". *36th AIAA/ASME/SAE/ASEE Joint Propulsion Conference, paper no. 2000-3350*, 2000.

[39] J. M. Cohen. *Private Communication*, 2000.

[40] O.J. Smith. "A controller to overcome dead time". *ISA Journal*, 6, 1959.

[41] A.Z. Manitius and A.W. Olbrot. Finite spectrum assignement problem for systems with delays. *IEEE Transactions on Automatic Control*, AC-24 no. 4, 1979.

[42] K. Ichikawa. Frequency-domain pole assignement and exact model-matching for delay systems. *Int. J. Control*, 41:1015–1024, 1985.

[43] W.A. Wolovich. *Linear Multivariable Systems*. Springer Verlag. Berlin, 1974.

[44] R. Ortega and R. Lozano. Globally stable adaptive controller for systems with delay. *International Journal of Control, Vol. 47, No. 1, pp 17-23*, 1988.

[45] S. I. Niculescu and A. M. Annaswamy. A simple adaptive controller for positive-real systems with time-delay. In *The American Control Conference in Chicago. IL., (to appear)*, February 2000.

[46] G.A. Baker and P Graves-Morris. *Padé Approximants*. 2nd edition, Cambridge University Press, 1996.

PAPER -23, J. P. Hathout

<u>Question (A. Banaszuk, USA)</u>

How effective is the Smith predictor-type controller if there is a large unmeasurable disturbance, such as turbulent velocity components driving the system? Don't you use the assumption that you know all the inputs during the delay block?

<u>Reply</u>

Robustness of Posi-Cast controllers has been analyzed in several publications. See, for example, references [41] and [45] in the paper.

<u>Question (J. Hermann, Germany)</u>

As you have shown, in a system with long time delay, there must be a long delay from activating the active control to achieving suppression of the oscillations. Applied to a realistic system, this may be too long. Can this problem be reduced?

<u>Reply</u>

The large delay τ_c is due to the fact that the secondary injection is at a certain distance upstream of the burning zone. This is a physical constraint that affects closed-loop control performance in general, regardless of the control algorithm. The implication of this constraint is that the effect of the control on the pressure will not take place for a minimum period of τ_c. After this period, the more sophisticated the controller, the smaller the settling time. The Posi-Cast control indeed results in the latter, as described in the presentation.

The time-delay effect may be reduced by introducing other actuating inputs closer to the burning zone. For example, it may be possible to introduce acoustic drivers or auxiliary fuel-injectors closer to the flame, which will not have the same time-delay constraint. The disadvantage of injection close to the flame may lie in the increase of emissions; an acoustic driver obviously avoids this problem, but may have limited authority. In either case, by designing a multi-input control strategy, where inputs closer to the flame act only over the time interval $[0, \tau_c]$, it may be possible to cope with the large delay.